May 11-15, 2008, Orlando, Florida, USA

ICONE16-48501

SCWR ROD BUNDLE THERMAL ANALYSIS BY A CFD CODE

M. Sharabi [(1)], W. Ambrosini [(1)], N. Forgione [(1)], S. He [(2)]

([1]) Dipartimento di Ingegneria Meccanica Nucleare e della Produzione, Università di Pisa, Via Diotisalvi 2, 56126 Pisa, Italy, Tel. +39-050-836673, Fax +39-050-836665, E-mail: walter.ambrosini@ing.unipi.it

([2]) School of Engineering, University of Aberdeen, Aberdeen AB24 3UE, United Kingdom, Tel. +44 (0)1224 272799, Fax. +44 (0)1224 272497, E-mail: s.he@abdn.ac.uk

ABSTRACT

The present paper describes the results of the application of the FLUENT code in the analysis of rod bundle configurations proposed for high pressure supercritical water reactors. The model considers a 1/8 slice of a rod bundle. The details from CFD calculations offer predictions of the circumferential clad surface temperature and of the effect of axial power distribution on the mass exchange between subchannels and on the maximum surface rod temperature. Geometry and boundary conditions are adopted from a previous work that made use of subchannel programs, allowing for a direct comparison between the two techniques. Both the standard k-ε model and the Reynolds stress transport model are used. Conclusions are drawn about the present capabilities in predicting heat transfer behavior in fuel rod bundles proposed for supercritical water reactors.

INTRODUCTION

Supercritical water reactors (SCWR) are considered in Generation IV as one of the promising nuclear reactor concepts to be commercialised in the next decades. Studies are ongoing worldwide in order to establish the most important design choices of a proposed plant whose main purpose is to achieve higher efficiency in power conversion. In fact, the use of water at supercritical pressures will benefit from using the well established PWR as well as fossil-fired supercritical steam generator technologies in the developments aiming at increasing the electrical power produced at the same thermal power [1-6].

Nevertheless, the presence of large variations in fluid properties in the vicinity of the pseudocritical temperature poses new problems to be tackled by detailed analyses. Heat transfer phenomena, like heat transfer enhancement and deterioration, observed at sufficiently low and high heat flux to mass velocity ratios, respectively, challenge the capabilities of both engineering correlations and CFD models [7-11].

Predictions of thermal-hydraulic conditions inside the fuel assembly of SCWRs are essential for providing information in support to design responding to safety requirements. Subchannel codes have been used to study thermal-hydraulic parameters for the complex fuel bundle configurations in SCWRs [12, 13]. The well-developed subchannel codes can treat complex geometries with flexibility to add additional channels such as moderator tubes. The effect of several design parameters on thermal-hydraulic behaviour in different subchannel configurations was investigated for both square and hexagonal fuel assemblies. Later, Waata et al. [14] developed a neutronic/thermal-hydraulic coupling procedure using the subchannel code STAFAS [12] with the Monte Carlo Code MCNP [15] to study the effect of water density variation on the neutron physics. This coupling is important due to the sharp decrease of water density between inlet and outlet and its strong link with the neutronic behaviour. They identified regions of higher and lower moderation in the fuel assembly and areas for design modifications, such as reduction of enrichment in corner pins.

Subchannel codes have anyway limited capabilities to handle two- and three-dimensional effects and are based on one-dimensional balance equations instead of solving the complete balance equations; heat transfer, turbulence, friction and mixing are evaluated from empirical closure correlations. On the other hand, CFD is considered as a powerful tool to overcome these deficiencies, by simulating realistically complicated three-dimensional geometries of fuel bundles. Yang et al. [16] used the STAR-CD commercial code [17] and adopted the standard k-ε turbulence model with wall function treatment to simulate the subchannels of the rod bundles. A great non-uniformity of the cladding temperature was found in the results of the square pitch assembly and it was attributed to the non-uniform distribution of the coolant within the subchannel cross section. They proposed a remedy for this problem from the heat transfer point of view, by incorporating a spacer structure to make more uniform the flow in the cross section area.

Laurien and Wintterle [18] simulated the flow in a short section of the High Performance Light Water Reactor (HPLWR) assembly using a second order closure to reproduce the secondary flows. The strength of the mean secondary flow vortices and the inter-channel mass transfer were identified.

The present paper describes the results of the application of the FLUENT code [19] in the analysis of rod bundle configurations proposed for high pressure supercritical water reactors. The model considers a 1/8 slice of a rod bundle. The details from CFD calculations will offer predictions of the circumferential clad surface temperature and of the effect axial power distribution on the exchange of mass between subchannels and on the maximum surface rod temperature, which is of great importance for safety considerations. Geometry and boundary conditions are adapted from Waata et al. [14] allowing for direct comparison between the two models.

PHYSICAL SYSTEM

Different assembly configurations were studied in previous studies for the thermal reactor option. Dobashi et al. [3] devised a hexagonal assembly with coolant flowing upwards, containing hexagonal water tubes with moderator flowing inside in the downward direction, to avoid mixing of the cold moderator with hot coolant in the upper plenum that would decrease the outlet core temperature. These water tubes are important to compensate for the large decrease in water density with heating. Control rods are inserted from the top into the water tubes. However, non-uniform radial power distribution resulted when this assembly design was included in the reactor concept by Squarer et al. [2].

On the other hand, Yamaji et al. [20] devised a square assembly design with square water tubes to solve this problem. In their design some rods contains Gadolinia which is used as a burnable poison to compensate for the excess of reactivity at the beginning of the cycle. A recent design which is also addressed in the European community is the one proposed by Hofmesiter et al. [21], which is based on the principle that each fuel rod should be neighbour to a moderator channel; the moderator to fuel ratio should be close to that in a PWR to optimize the power density, and the ratio of structural materials to fuel should be minimum to minimize the fuel enrichment.

One-eighth of this assembly is shown in Figure 1. It is divided into seven fuel rods and nine subchannels as illustrated in the figure. The same geometry parameters and operating conditions as in Waata et al. [14] are adopted in the current study to allow for direct comparison between the detailed models of CFD calculations and the simplified subchannel code adopted in their study. They can be summarized as the following:

- Assembly: 7×7 fuel elements
- Fuel element diameter: 8.0 mm
- Pitch between fuel elements: 9.2 mm
- Gap between fuel rod and wall: 1 mm
- Active height: 4.2 m
- System pressure: 25 MPa
- Inlet temperature: 280 ^{o}C
- Total mass flow rate in one assembly: 0.167 kg/s
- Mass flow rate in the water tube: 0.0139 kg/s
- Mass flow rate between assembly boxes: 0.0278 kg/s
- The water tube in Figure 1 replaces nine fuel elements.

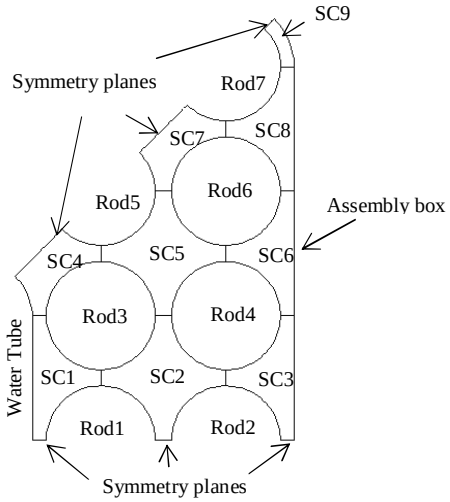

Figure 1. One-eight of the SCWR fuel assembly addressed in this work.

The linear power distributions in each one of the fuel rods, as obtained by the coupled calculations of Waata et al. [14], are shown in Figure 2.

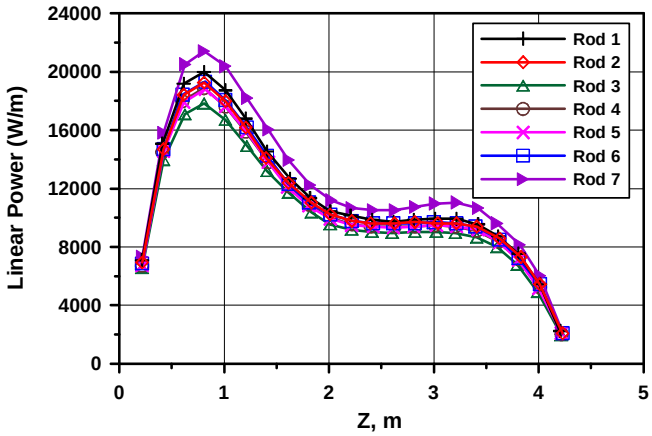

Figure 2 Linear power distribution along each fuel rod (Waata et al. [14])

COMPUTATIONAL METHODS

In the work by Yang et al. [16], wall functions were used to address the problem of heat transfer at supercritical pressure, making comparisons with experimental data from Yamagata et al. [7] for circular tubes. It was found that the wall function approach is able to reproduce the wall temperature fairly well when the buoyancy force is not significant. On the other hand, the wall function approach is

not able to predict the deterioration in heat transfer when buoyancy effects become important [22].

In this work, due to the large computational domain, the wall functions approach is adopted to avoid using very fine mesh in the near wall region. Two turbulence models are considered; the Standard k-ε model and the Reynolds stress model (RSM) both with the wall functions approach. Although the power peaks shown in Figure 2 are large enough with respect to the mass velocity to lead to heat transfer deterioration, this effect will not be considered in the current study.

The whole bundle geometry shown in Figure 1 is discretized using a mesh having the dimensionless distance y^+ of the first node beside the wall greater than 30 throughout the domain. A cross sectional view of the grid for subchannel SC5 is shown in Figure 3. This mesh topology is repeated in every subchannel; 160 uniform grid points are used in the axial direction. Each subchannel can be treated as a separate volume that interacts with other subchannels through common faces.

The linear power distributions shown in Figure 2 are applied as wall boundary conditions for the energy equation at the surface of the fuel rods. This is implemented in a user defined function file which is linked to the Fluent code. Adiabatic boundary conditions are assumed at the assembly box and the water tube. Uniform profiles of all the dependent variables are assumed at the assembly inlet. The turbulent intensity at the inlet is set to 7%, as a reasonable assumption having low impact on heat transfer along the channel. A pressure boundary condition is applied at the outlet plane. The NIST standard reference database 23, version 7 [23], is used to generate tables of density, specific heat, thermal conductivity and viscosity as a function of temperature. These tables are used within the FLUENT to account for the variation of fluid properties with temperature. The variation with pressure is ignored in this work since the pressure drop along the assembly is small.

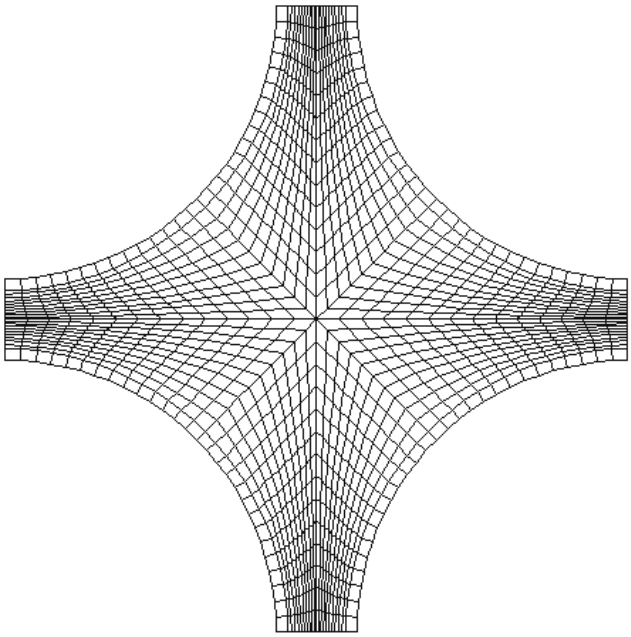

Figure 3 Plane view of the mesh for the SC5

The SIMPLEC algorithm is adopted for the pressure-velocity coupling together with the body force weighted discretization scheme, which is particularly recommended for the case of buoyant flows. Dependence of the solution on the convection scheme has been checked by considering both the first and the second-order upwind scheme. The convergence tolerance was set to be 10^{-7} based on the normalized residuals for all the dependent variables.

RESULTS AND DISCUSSIONS

The mixing between different subchannels can be visualized by plotting the mass velocity in each subchannel. Figure 4 and Figure 5 show the mass velocity distribution in each subchannel as predicted by the *k-ε* model and the RSM model, respectively. It can be noted that, although the same mass velocity is provided to subchannels at the inlet, the mass velocity of subchannel SC9 decreases largely compared to other subchannels due to the high flow resistance at the corner. In addition, no significant difference between the predictions from the two different turbulence models are observed, suggesting that the secondary flow that can be predicted by the RSM model does not play a significant role in the mixing between subchannels. The secondary flow near the outlet section of SC5 is depicted in Figure 6 showing the formation of eight confined vortices inside the subchannel.

The distributions of the bulk temperatures as predicted by the two adopted turbulence models in each subchannel are shown in Figure 7 and Figure 8. It is seen that no significant difference is observed in the prediction by the two turbulence models. The average clad surface temperature in each subchannel as predicted by the standard *k-ε* turbulence model is shown in Figure 9. The same predictions from the Waata et al. [14] calculations for the bulk and clad surface temperature are shown in Figure 10 and Figure 11, respectively.

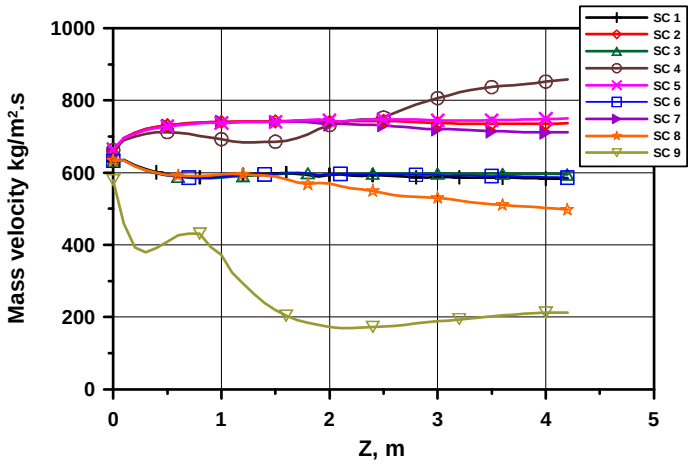

Figure 4 Mass velocity distribution in each subchannel as predicted by the *k-ε* model.

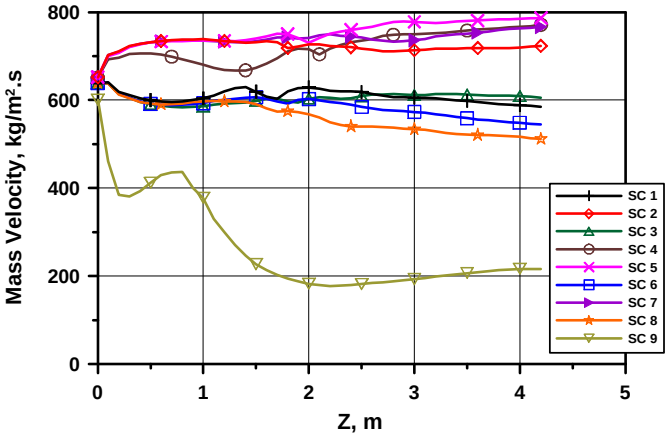

Figure 5 Mass velocity distribution for every subchannel as predicted by the RSM model

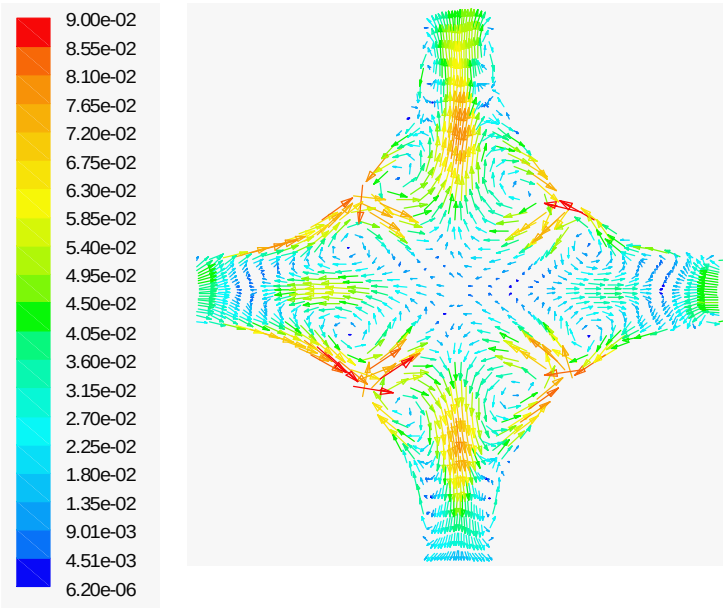

Figure 6. Secondary flow distribution as predicted by the RSM model for SC5

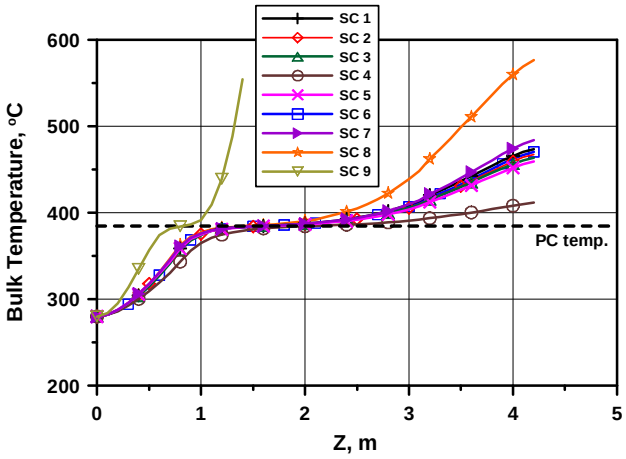

Figure 7. Bulk temperature distribution in each subchannel as predicted by the *k-ε* model

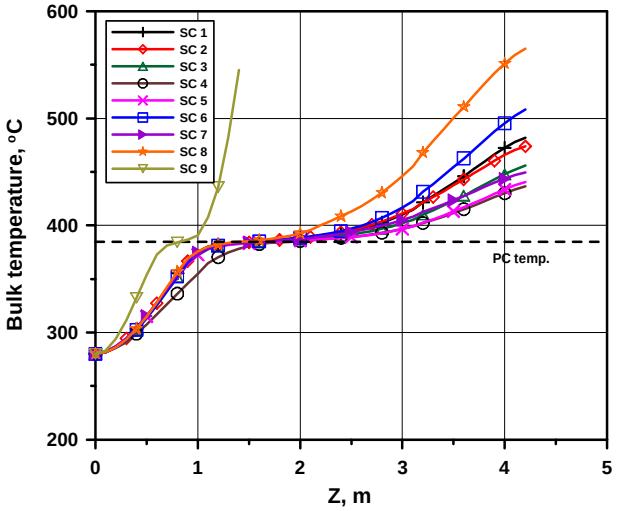

Figure 8. Bulk temperature distribution in each subchannel as predicted by the RSM model

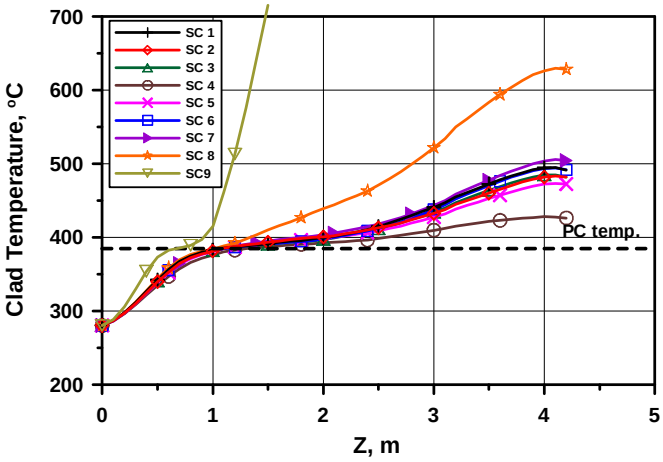

Figure 9. Average clad temperature distribution as predicted by the *k-ε* model

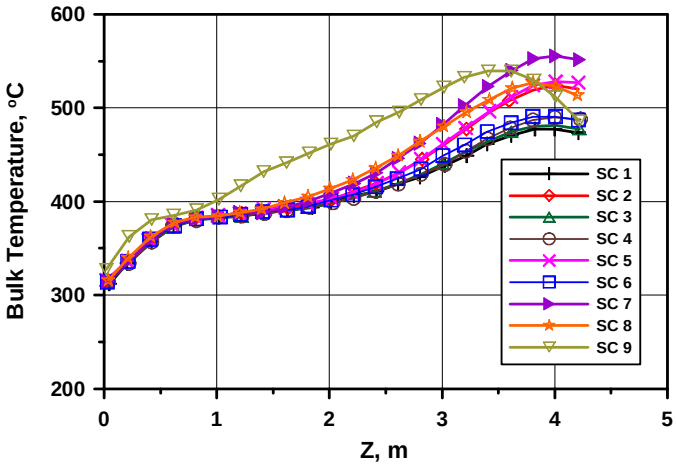

Figure 10. Bulk temperature distribution in each subchannel (from Waata et al. [14])

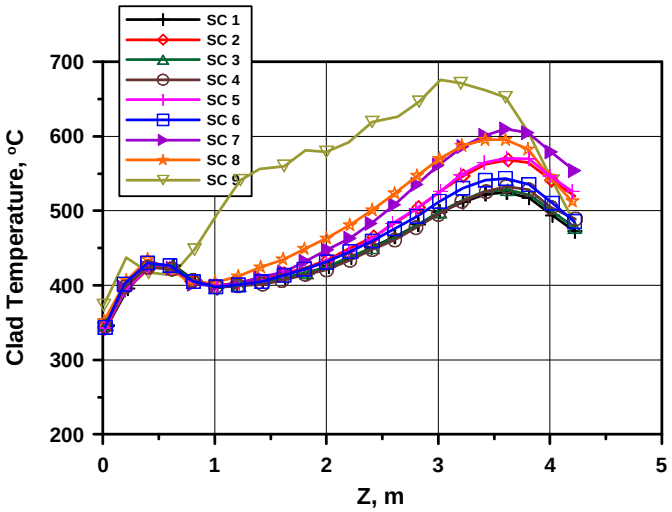

Figure 11. Clad temperature distribution in each subchannel (from Waata et al. [14])

The peak on the clad temperature predicted by the subchannel model appears also in the local distributions of the clad surface temperature (not shown here); however, it has been smoothed out in the averaging process and therefore not clear in the CFD averaged distributions. The distributions from the two codes have the same general trend. As it is seen when the wall temperature approaches the pseudocritical temperature, the increase of the clad surface temperature becomes very low indicating enhancement of heat transfer effectiveness as a result of the sharp peak in the specific heat at the pseudocritical temperature. On the other hand, the clad surface temperature of the rod number 9 achieves a very high value (partly shown in the figures) due to the strong decrease in the mass velocity. The subchannel code predicted the SC9 to be the hottest channel, however, the increase of the wall temperature is not as large as in the CFD calculations. This suggests that the exchange of mass between different subchannels is represented in a rather different way by the subchannel code.

A remedy for this problem can be achieved by reducing the power of the corner rod (Rod9). In the current study, the power distribution used for Rod9 in Figure 2 is multiplied by a factor of 0.5. This is found sufficient to reduce the maximum clad temperature below 620 °C which is the design temperature limit for the cladding material [1]. The bulk and average clad surface temperatures at these new conditions are shown in Figure 12 and Figure 13, respectively. Distributions of the transversal velocity contours at different axial locations are shown in Figure 14 and Figure 15. Some differences in the mass velocity distributions with these new conditions are observed because of the change in the density distribution; however the distributions are not repeated here.

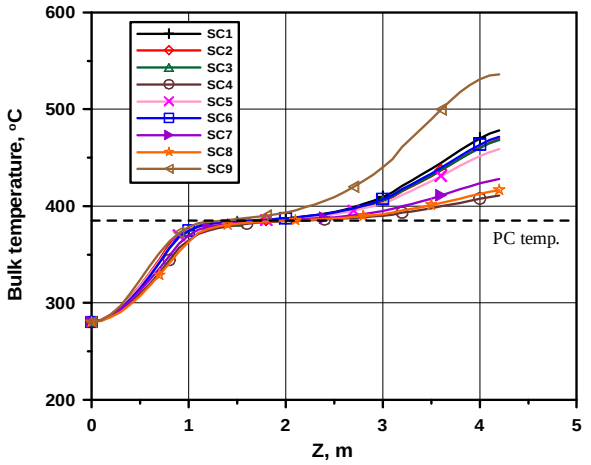

Figure 12. Bulk temperature distribution in each subchannel as predicted by the k-ε model

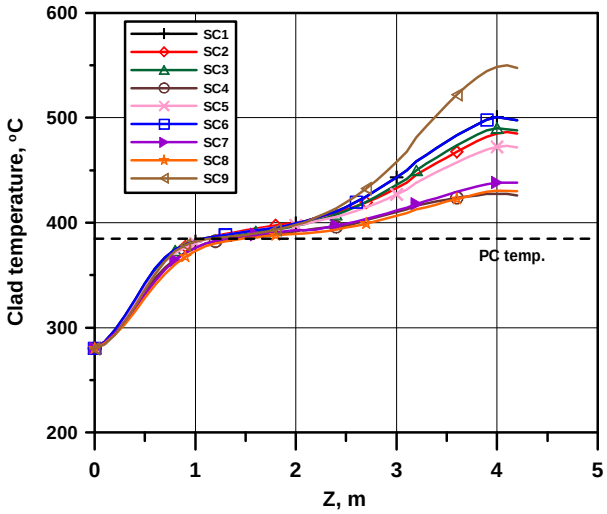

Figure 13. Average clad temperature distribution as predicted by the k-ε model

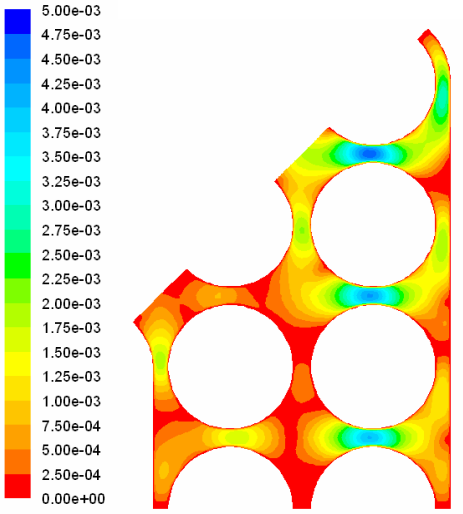

Figure 14. Transversal velocity contours at 0.2 m from the inlet plane as predicted by the standard k-ε turbulence model

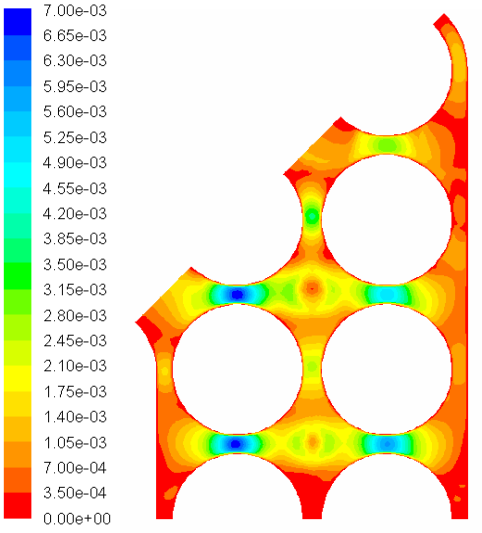

Figure 15. Transversal velocity contours at 2 m from the inlet plane as predicted by the standard *k-ε* turbulence model

The distributions of heat transfer coefficient are shown in Figure 16 indicating clearly the heat transfer enhancement at the location where the wall temperature exceeds the pseudocritical temperature. The SC9 shows a higher heat transfer coefficient due to the tendency of the *k-ε* turbulence model with wall functions to overestimate the heat transfer coefficient at high heat flux to mass velocity ratios.

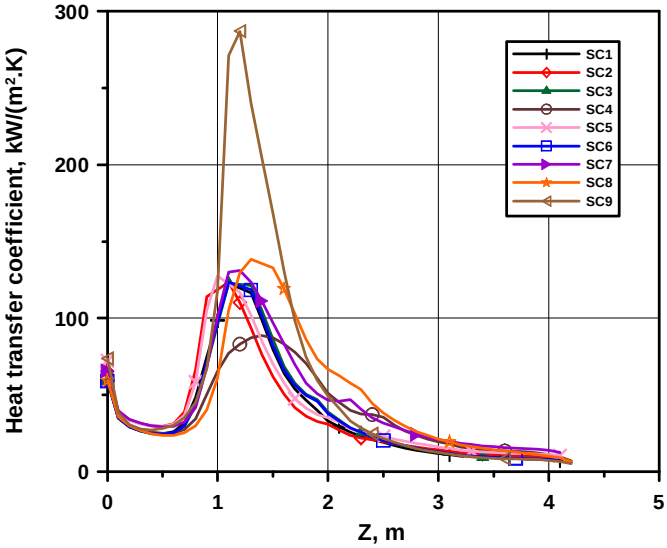

Figure 16 Heat transfer coefficient distribution in each subchannel as predicted by the *k-ε* model

The local distribution of the circumferential surface clad temperature for different fuel rods and at different axial locations are shown in

Figure 17 to Figure 19. The angle is measured starting from the positive *x*-axis and in counter clockwise direction. Strong temperature gradients are observed with the maximum temperature occurring close to the tight gap between two fuel rods. The temperature variations increase with the increase of the distance from the inlet section. The Rod3 shows the lowest temperatures on the side that faces the water tube. Also for Rod6, on the side that faces Rod7, the temperature is lower because of the lower power generation by Rod7. Rod7 shows high temperature distribution in the gap of SC9, however its surface temperature distribution on SC8 is lower due to its lower power.

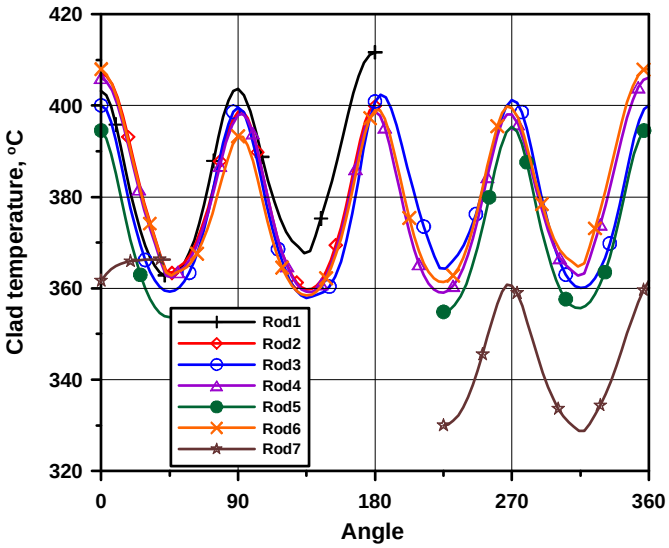

Figure 17 Circumferential clad temperature distributions at 0.5 m from the inlet plane as predicted by the standard *k-ε* turbulence model

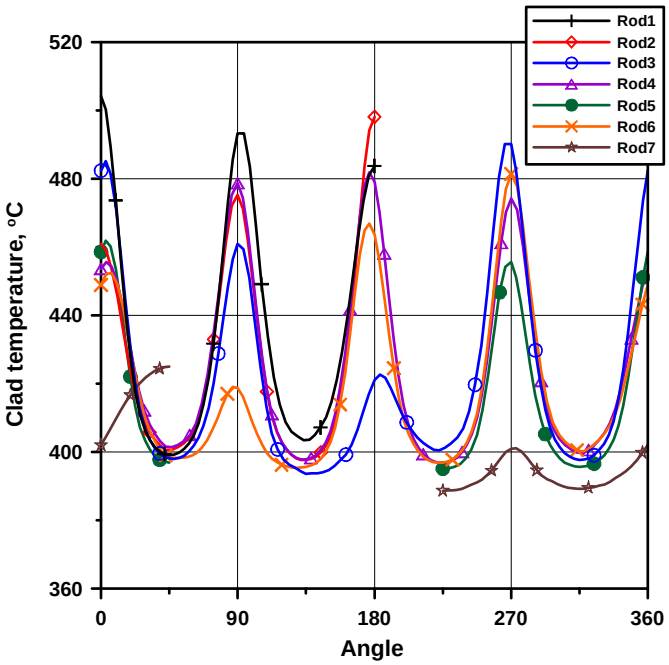

Figure 18 Circumferential clad temperature distributions at 2 m from the inlet plane as predicted by the standard *k-ε* turbulence model

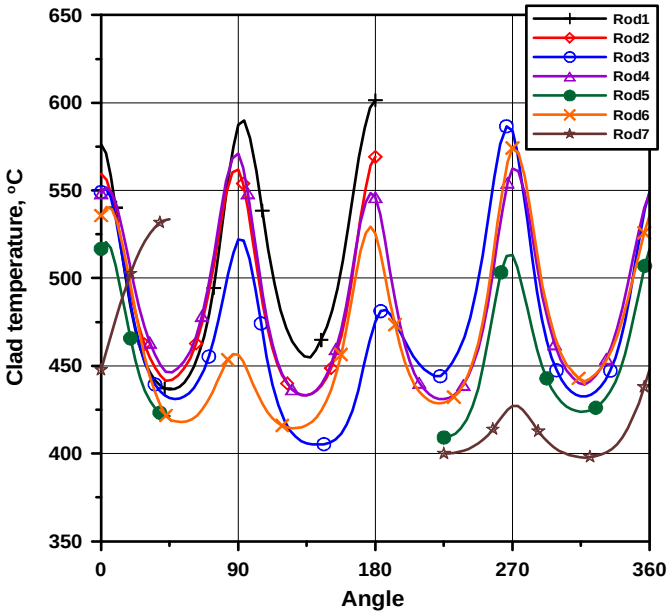

Figure 19 Circumferential clad temperature distributions at 3 m from the inlet plane as predicted by the standard k-ε turbulence model

CONCLUSIONS

The calculations performed in this work showed that CFD predicts details in mass flux distribution among subchannels in a different way with respect to predictions by subchannel approaches. This requires careful analyses to be made by both techniques in order to discuss the relevant aspects influencing heat transfer from fuel rods.

As it was seen, the use of the standard k-ε model and of the Reynolds stress model with wall functions provided nearly the same results for flow distribution and rod cladding temperature. This shows that, within the limitations of the wall function approach, details of the secondary flows occurring in the cross section of the subchannels have a limited impact on mass transfer between the subchannels.

Previous experience in the use of low-Reynolds number models, even in simple configurations, showed that the onset of heat transfer deterioration can be correctly predicted, though the consequent wall temperature rise is generally overestimated. In the case of rod bundles, the application of low-Reynolds number models is interesting, though there is a basic uncertainty about the relevance of heat transfer deterioration in the presence of turbulence generation by spacer grids.

Clarifying these aspects is necessary for a proper design of fuel bundles for supercritical water reactors and provides the matter for further studies.

REFERENCES

[1] Schulenberg T. and Starflinger J., 2007: "Core Design Concepts for High Performance Light Water Reactors," Int. J. Nuclear Engineering and Technology, Vol. 39, No. 4.

[2] Squarer D., Schulenberg T., Struwe D., Oka Y., Bittermann D., Aksan N., Maraczy C., Kyrki-Rajamäki R., Souyri A. and Dumazh P., 2003: "High performance light water reactor," Nuclear Engineering and Design, vol. 221, pp 167–180.

[3] Dobashi, K., Oka, Y. and Koshizuka, S., 1998: "Conceptual design of a high temperature power reactor cooled and moderated by supercritical light water," Proceedings of the Sixth International Conference on Nuclear Engineering. ICONE6, ASME, NY.

[4] Heusener G., Mueller U. and Squarer D., 2000: "High performance light water reactor (HPLWR)," Nucl. Europe Worldscan XX (1/2), 59–60.

[5] Heusener G., Mueller U., Schulenberg T. and Squarer D., 2000: "European development program for a high performance light water reactor (HPLWR)," SCR-2000, The University of Tokyo, Tokyo, Japan.

[6] Oka Y., 2000: "Review of high temperature water and steam cooled reactor concepts," Proceedings of the First International Symposium on Supercritical Water-cooled Reactors. Design and Technology, SCR-2000, The University of Tokyo, Tokyo, Japan.

[7] Yamagata K., Nishikawa K., Hasegawa S., Fujii T. and Yoshida S. 1972: "Forced Convection Heat Transfer to Supercritical Water Flowing in Tubes," Int. J. Heat Mass Trans. 15, 2575-2593.

[8] Pioro L.I., Khartabil H. and Duffey R.B. 2004: "Heat Transfer to Supercritical Fluids Flowing in Channels-Empirical Correlations (Survey)," Nuclear Engineering and Design, 230, 69-91.

[9] Cheng X. and Schulenberg T., 2001: "Heat Transfer at Supercritical Pressures – Literature Review and Application to an HPLWR," Forschungzentrum Karlsruhe, FZKA 6609.

[10] He S., Kim W.S., Jiang P.X., and Jackson J.D. 2004: "Simulation of Mixed Convective Heat Transfer to Carbon Dioxide at Supercritical Pressure," J. Mech. Eng. Sc., 218, 1281-1296.

[11] Yang J., Oka Y., Ishiwatari Y. Liu J. and Yoo J., 2007: "Numerical Investigation of Heat Transfer in Upward Flows of Supercritical Water in Circular Tubes and Tight Fuel Rod Bundles," Nucl. Eng. & Des., 237, pp. 420-430.

[12] Cheng X, Schulenberg T., Bittermann D. and Rau P., 2003: "Design Analysis of Core Assemblies for Supercritical Pressure Conditions," Nuclear Engineering and Design, Vol. 233, pp. 279-294.

[13] Yoo J. Oka Y., Ishiwatari Y., Yang J. and Liu J., 2007: "Subchannel Analysis of Supercritical Light Water-Cooled Fast Reactor Assembly," Nuclear Engineering and Design, Vol. 237, pp. 1096-1105.

[14] Waata C., Schulenberg T., Cheng X., and Laurien E., 2005: "Coupling of MCNP with a Subchannel Code for Analysis of a HPLWR Fuel Assembly," Proc. of NURETH-11, Avignon, France.

[15] Briesmeister J.F., 2000: "A general Monte-Carlo N Particle Transport code," Version LA-1370-M.

[16] Yang J., Oka Y., Ishiwatari Y. Liu J. and Yoo J., 2007: "Numerical Investigation of Heat Transfer in Upward Flows of Supercritical Water in Circular Tubes and Tight Fuel Rod Bundles," Nucl. Eng. & Des., 237, pp. 420-430.

[17] CD-Adapco, 2005: "STAR-CD Version 3.26 Manuals".

[18] Laurien E. and Wintterle T., 2007: "Secondary Flow in the Cooling Channels of the High-Performance Light Water Reactor," Proc. of ICAPP 2007, Nice, France.

[19] FLUENT 6.2.16 (2005): "Users Guide," FLUENT Inc.

[20] Yamaji A., Oka Y. and Koshizuka S., 2001: "Conceptual Core Design of a 1000MWe Supercritical Pressure Light Water Cooled and Moderated Reactor," ANS/HPS Student Conf. Texas, A&M University.

[21] Hofmeister J., Schulenberg T. and Starflinger J., 2005: "Optimization of a Fuel Assembly for a HPLWR," Paper 5077, Proc. ICAPP 05, Seoul, Korea.

[22] Seo K.W., Anderson M.H., Corradini, M.L., Oh B.D., and Kim M.H., 2004: Studies of Supercritical Heat Transfer and Flow Phenomena, Nureth-11, Avignon, France.

[23] NIST, 2002, Reference Fluid Thermodynamic and Transport Properties – REFPPRO, Aug. (2002), Lemmon, E.W., McLinden, M.O., Hurber, M.L. (Eds.), NIST Standard Reference Database 23 (Software and Source), V. 7.0, U.S. Department of Commerce.